ADVANCED FUNCTIONAL MATERIALS
www.afm-journal.de

Modulating the Properties of Azulene-Containing Polymers through Controlled Incorporation of Regioisomers

Kazuhiko Tsurui, Masahito Murai, Sung-Yu Ku, Craig J. Hawker, and Maxwell J. Robb**

Two libraries of random conjugated polymers are presented that incorporate varying ratios of regioisomeric azulene units connected via the 5-membered or 7-membered ring in combination with bithiophene or fluorene comonomers. It is demonstrated that the optoelectronic and stimuli-responsive properties of the materials can be systematically modulated by tuning the relative percentage of each azulene building block in the polymer backbone. Significantly, these materials exhibit stimuli-responsive behavior in the solid state with spin-coated thin films undergoing rapid and reversible color switching. Ultimately, this work introduces a new design strategy in which the optoelectronic properties of conjugated polymers can be modulated by varying only the regiochemistry of the constituent building blocks along a polymer chain.

1. Introduction

The potential of conjugated polymers for use in organic electronic devices including photovoltaics (OPVs),[1–4] field effect transistors (OFETs),[5,6] and light-emitting diodes (OLEDs)[7] has motivated the development of a diverse range of molecular building blocks that has allowed a vast array of conjugated polymers to be prepared.[8] Fine-tuning of the electronic and molecular structure of these units has led to major advances in charge transport and optoelectronic characteristics. Some of the most successful building blocks include diketopyrrolopyrrole (DPP),[9–13] isoindigo,[14–16] thienopyrrolodione (TPD),[17–19] and benzodithiophene (BDT),[20–22] all of which contain a heterocyclic framework that can be further derivatized for control of both electronic structure and morphology in the solid state.

An alternative building block that has received significantly less attention is azulene which comprises a purely hydrocarbon structure and possesses a range of unique properties. Unlike its constitutional isomer, naphthalene, azulene is a bright blue compound that exhibits large dipolar character (1.08 D) due to resonance delocalization that results in an electron-rich 5-membered ring and an electron-poor 7-membered ring.[23–25] The unique photophysical properties of azulene arise from a dissimilar distribution of electron density between the HOMO and LUMO leading to a relatively small electron repulsion energy in the first excited singlet state.[25] These attributes, coupled with its stimuli-responsive behavior in acidic environments, make azulene a promising building block for the construction of new conjugated polymers with unique properties.[26–29]

Responsive materials that exhibit dramatic changes in optical properties upon the introduction of external stimuli are promising for a number of applications including sensing technologies.[30–32] In the case of azulene-containing materials, protonation leads to the formation of a stable tropylium cation with significantly different spectroscopic properties than the neutral species.[33–36] Despite its potential, most materials incorporating azulene as a building block have been limited to functionalization by various electrophilic transformations, leading to oligomers and polymers with the azulene nucleus connected exclusively through the 5-membered ring (1,3-connectivity).[37–43] We recently demonstrated that azulene-based materials connected through the electron-poor 7-membered ring (4,7-connectivity) exhibit unique properties, in part due to the conservation of π-conjugation after protonation.[44,45] Building on these findings, the combination of both the 1,3- and 4,7-regioisomers of azulene could have important implications for materials design. In analogy to random D–A copolymers that comprise multiple types of randomly distributed donor and/or acceptor units,[13,46–52] we hypothesized that conjugated polymers with tunable electronic properties could be accessed by incorporation of different regioisomeric azulene building blocks in which their connectivity (electron-rich or electron-poor 5- and 7-membered rings) is varied along the polymer chain.

Herein, we describe the synthesis and evaluation of a series of random copolymers incorporating the azulene building block with varying ratios of 1,3- and 4,7-connectivity. Both bithiophene and fluorene comonomers were investigated leading to two new libraries of random conjugated copolymers. Significantly, we demonstrate that the optoelectronic properties

K. Tsurui, Dr. S.-Y. Ku, Prof. C. J. Hawker, Dr. M. J. Robb
Department of Chemistry and Biochemistry
Materials Department,
and Materials Research Laboratory
University of California
Santa Barbara, California 93106, USA
E-mail: hawker@mrl.ucsb.edu; max@mrl.ucsb.edu
Dr. M. Murai
Division of Chemistry and Biotechnology
Graduate School of Natural Science and Technology
Okayama University
3–1–1 Tsushimanaka, Kita-ku, Okayama 700–8530, Japan

DOI: 10.1002/adfm.201402554

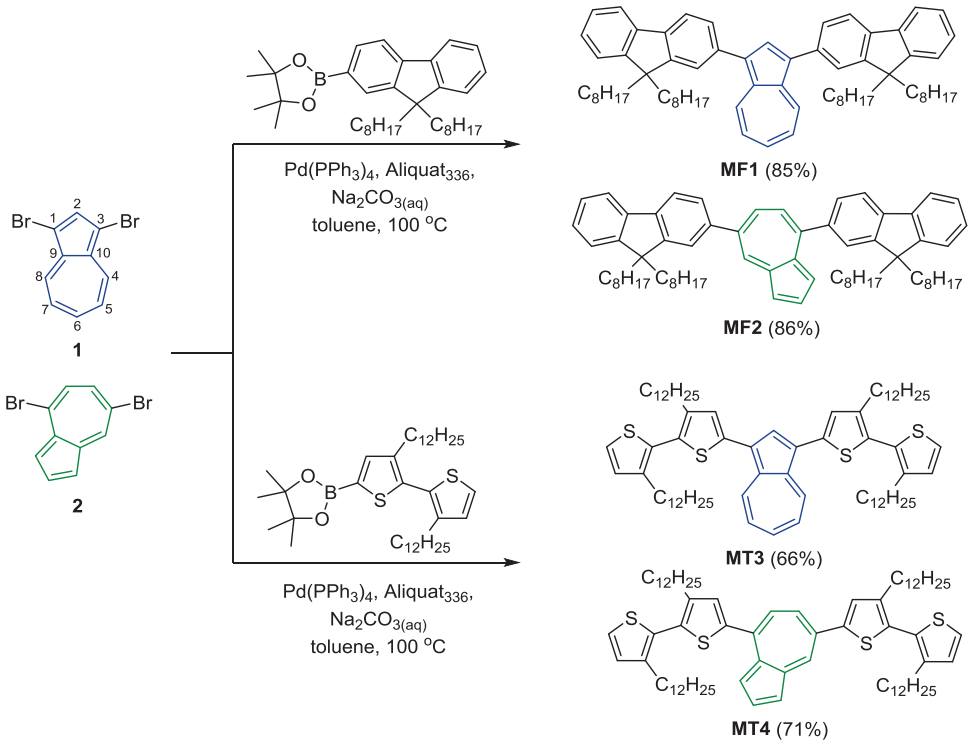

Scheme 1. Synthesis of 1,3- and 4,7-disubstituted model compounds **MF1**, **MF2**, **MT3**, and **MT4**.

of these polymers can be varied systematically by changing the incorporation of regioisomeric azulene units in the polymer backbone. Of particular note is the stimuli-responsive behavior of these materials in both solution and the solid state, making them interesting candidates as dopable active materials for sensing and other organic electronic device applications. Ultimately, this work represents a new design strategy in which the optoelectronic properties of conjugated polymers can be modulated by simply varying the regiochemistry of the constituent building blocks along the polymer backbone.

2. Results and Discussion

We initially synthesized several small molecule model compounds to compare the effect of regioisomerism of the azulene building block on the physical properties derived from connectivity through either the 5-membered or 7-membered ring (**Scheme 1**). Molecules **MF1** and **MF2** incorporate a central azulene unit flanked with fluorene substituents connected at the 1,3- or 4,7-positions of azulene, respectively. Additionally, **MT3** and **MT4** incorporate bithiophene substituents appended to either the 5-membered or 7-membered ring of a central azulene core. The model compounds were synthesized by Suzuki-Miyaura cross-coupling with 1,3-dibromoazulene[53] **1** or 4,7-dibromoazulene[44] **2** and mono-borylated fluorene or bithiophene derivatives containing solubilizing alkyl groups. The addition of a few drops of Aliquat 336 improved the reactions with all compounds isolated in moderate to very good yield (66–86%). The structures of the model compounds were confirmed by ^{1}H and ^{13}C NMR spectroscopy, IR spectroscopy, and mass spectrometry. The asymmetry resulting from connectivity at the 4,7-positions of the 7-membered ring of azulene is clearly reflected in the ^{1}H NMR spectrum of **MT4** which exhibits two unique singlets at 7.29 and 7.46 ppm for the protons at the 4,4′-positions on the internal thiophene moieties (**Figure 1**). In contrast, these protons appear as one singlet at 7.18 ppm in the ^{1}H NMR spectrum of the symmetrical compound **MT3.** A similar affect is observed for **MF2** in which the protons at the 1,1′-positions of the fluorene substituents appear as two unique resonances in contrast to one doublet observed for **MF1**. More importantly, the resonances corresponding to the bithiophene and fluorene substituents are shifted downfield in the ^{1}H NMR spectra of **MF2** and **MT4** compared to **MF1** and **MT3**, which is indicative of the acceptor character of the azulene nucleus when connected at the 4,7-positions of the electron-deficient 7-membered ring.

The optical and stimuli-responsive properties of the model compounds were subsequently investigated by UV–Visible spectroscopy with the structural changes between the four compounds being qualitatively different as noted by their variation in color and clearly demonstrating that the regiochemistry of the central azulene unit significantly affects the optoelectronic properties (**Figure 2**a). The absorption spectra of **MF1** and **MT3** with the azulene unit connected at the 1,3-positions of the 5-membered ring exhibit a broad profile with little fine structure while **MF2** and **MT4** with the azulene nucleus substituted at the 4,7- positions on the 7-membered ring display two distinct absorption maxima. This spectral region with onsets of absorption between 420 and 475 nm corresponds to the S_0–S_2 transition with increased conjugation length resulting in an energy gap that is lower by 0.5–0.9 eV compared to the

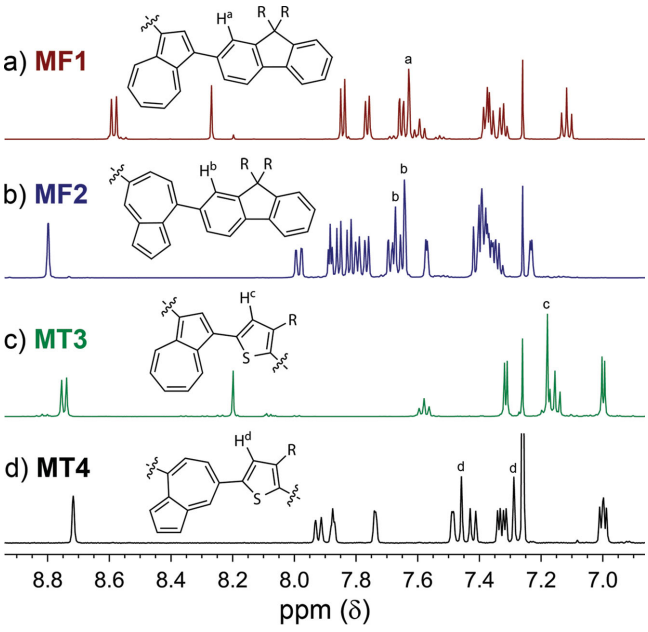

Figure 1. ^{1}H NMR spectra ($CDCl_3$, 600 MHz) of model compounds a) **MF1**, b) **MF2**, c) **MT3**, and d) **MT4**. Resonances corresponding to protons at the 1(1′)-fluorenyl positions of **MF1**/**MF2** and the 4(4′)-thienyl positions of **MT3**/**MT4** are labeled.

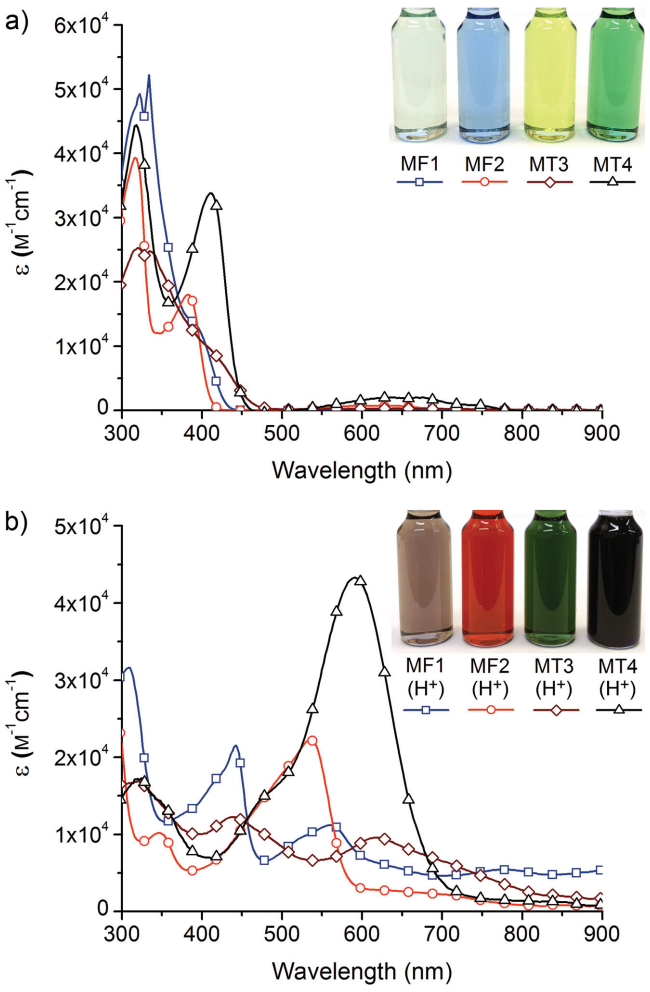

Figure 2. UV–Visible absorption spectra of model compounds in a) HCl_3 and b) $CHCl_3$/TFA (30% TFA by volume). Insets show optical photographs of the model compound solutions with a concentration of 1×10^{-4} M.

parent azulene.[25,54] Similar trends have been observed for other conjugated azulene oligomers.[28,35,44] In addition, each of the model compounds exhibit broad absorptions centered at approximately 650 nm characteristic of the S_0–S_1 transition of azulene.[55]

The stimuli-responsive properties of azulene are a key motivation for its incorporation into conjugated materials. In the presence of strong acids, protonation of the 5-membered ring of azulene leads to the formation of an aromatic, 6π–electron tropylium cation. This stimuli-responsive behavior was demonstrated for the model compounds upon protonation with trifluoroacetic acid (TFA) with dramatic changes in the UV–Visible spectra and solution color being observed (Figure 2b). The absorption spectra of **MF1** and **MT3** exhibit broad, multimodal profiles while **MF2** and **MT4** have distinct absorptions with maxima at 535 nm and 593 nm, respectively. The influence of regiochemistry and substitution is most dramatic for the case of **MT4** where the more strongly donating bithiophene moieties can directly stabilize the cationic 7-membered ring of the azulene core. Changes to the absorption spectra saturated after addition of ~30% TFA (v/v) to solutions of the model compounds in chloroform with changes in absorption being less pronounced when the experiments were performed using tetrahydrofuran (THF) as solvent.[41]

To gain additional insight into the effects of substitution and regiochemistry on the electronic structure and photophysical properties of the model compounds, density functional calculations were performed at the B3LYP/6–31G* level of theory (calculations for **MT3** and **MT4** are shown in **Figure 3**; for **MF1** and **MF2**, see Figure S1 in the Supporting Information). To simplify the calculations, truncated structures were optimized in which the dodecyl (bithiophene) and octyl (fluorene) chains were replaced with methyl groups. In their neutral state, the HOMO of **MF1** and **MT3** is delocalized over the entire molecule which is reflective of the donating ability of the azulene unit connected through the electron-rich 5-membered ring. Additionally, the LUMO is localized on the azulene core which reflects the electronic isolation of the electron-poor 7-membered ring from the π-system of the fluorene and bithiophene donor substituents. In contrast, the LUMO of **MF2** and **MT4** is partially delocalized from the central azulene nucleus onto the fluorene and bithiophene moieties indicating donation of the substituent π-system into the electron-poor 7-membered ring of azulene. The increased electron donating ability of the bithiophene substituents was found to more effectively stabilize the LUMO compared to fluorene substituents while 4,7-regiochemistry leads to a deeper HOMO for both **MF2** and **MT4**. Optimized geometries indicate that both the fluorene and bithiophene substituents are rotated significantly out of plane with respect to the azulene core, although to a slightly less extent for **MF1** and **MT3** connected through the 5-membered ring of azulene. The less effective π-conjugation in azulene

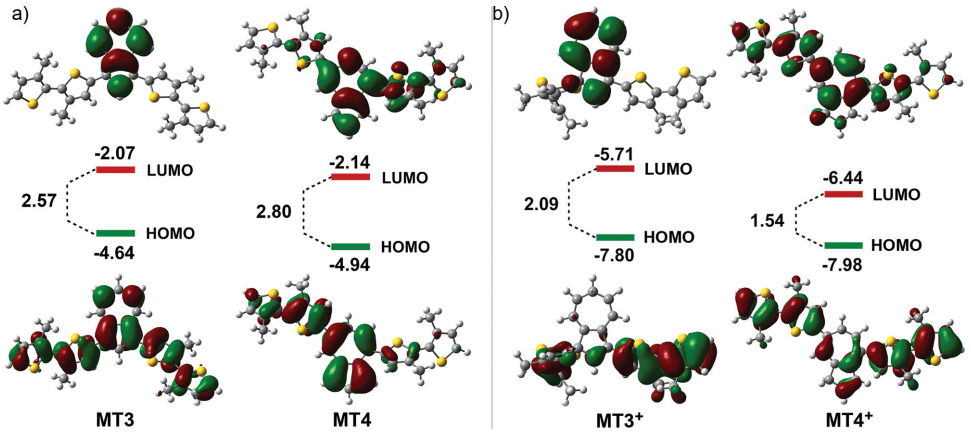

Figure 3. Optimized structures and contour plots of frontier molecular orbitals and energies for model compounds **MT3** and **MT4** in their a) neutral and b) protonated state calculated by DFT at the B3LYP/6–31G* level of theory.

derivatives with 4,7-regiochemistry is reflected in their slightly larger HOMO–LUMO energy gap in the neutral state. These predictions are also consistent with the UV–Visible absorption spectra in Figure 2.

DFT calculations were also performed for the protonated model compounds to gain insight into the changes observed in the UV–Visible spectra and their stimuli-responsive behavior (Figure 3b and Figure S1). It is important to note that these calculations are for molecules in the gas phase and provide qualitative guidance of the excited state properties of the charged species. The fluorene and bithiophene substituents were shown to have a pronounced effect on the electronic structure of the protonated model compounds, particularly for the 4,7-substituted azulene derivatives. In general, protonation of azulene significantly lowers the HOMO and LUMO energy levels for all of the model compounds with decreased bandgaps also being observed; however, the effect of protonation for compounds with 4,7-regiochemistry is considerable, resulting in calculated bandgaps of 1.62 eV and 1.54 eV for **MF2**$^+$ and **MT4**$^+$, respectively (cf. to 3.03 eV and 2.80 eV for the neutral species). This significant reduction in bandgap is due to stabilization of the LUMO by the electron donating ability of the fluorene and bithiophene substituents directly connected to the cationic 7-membered ring of the azulenium core. Furthermore, the HOMO of the protonated species is largely localized on the electron-donating fluorene and bithiophene moieties; however, like the neutral state calculations, the LUMO is confined to the azulene core for **MF1**$^+$ and **MT3**$^+$ while it is more delocalized for **MF2**$^+$ and **MT4**$^+$. The distinct separation of the HOMO–LUMO topology for **MF1**$^+$ and **MT3**$^+$ in the protonated state is likely responsible for their absorption into the near-IR region as a result of significant intramolecular charge transfer (ICT).[35] Protonation of azulene was also predicted to decrease the dihedral angles between azulene and the fluorene or bithiophene substituents for **MF2**$^+$ and **MT4**$^+$ with 4,7-regiochemistry while the dihedral angles for **MF1**$^+$ and **MT3**$^+$ were predicted to increase compared to the neutral species. The latter effect is due to the fact that protonation occurs at the 1,3-positions of azulene, causing a change from sp^2 to sp^3 hybridization at that carbon center. These results suggest that, while protonation may lead to enhanced π-conjugation for connectivity through the 7-membered ring of azulene, increased ICT may also benefit the absorption properties of materials connected via the 5-membered ring. Hence, a combination of the two regiochemistries may be advantageous as a design strategy toward new responsive materials.

Encouraged by the results of the small molecule investigation, we set out to prepare a library of conjugated polymers based on the same structural motifs used for the model compounds. In comparison to previous work on random conjugated polymers, we envisaged that materials with varied optoelectronic properties could be accessed through copolymerization of multiple monomer units; however, instead of using significantly disparate building blocks, the electronic and structural properties of the polymers could be tuned simply by varying the regiochemistry of the azulene units along the polymer chain. Accordingly, two series of conjugated polymers were synthesized incorporating varying ratios of azulene repeating units connected through the 5-membered or 7-membered ring with either fluorene or bithiophene comonomers via Pd-catalyzed polycondensation methods (**Scheme 2**). For the first series (**PF1–PF5**), the commercially available 9,9-dioctylfluorene-2,7-diboronate monomer **3** was copolymerized with varying feed ratios of **1** and **2** under Suzuki-Miyaura cross-coupling conditions using Pd_2dba_3 and P(*o*-tol)$_3$ in toluene at 85 °C with tetraethylammonium hydroxide as a boron-activating base.[56] It should be noted that **PF1** has been reported previously.[41] A second polymer series (**PT1–PT5**) was also prepared, again reacting varying feed ratios of dibromoazulene regioisomers **1** and **2** with bis-stannylated bithiophene monomer **4** under Stille cross-coupling conditions using Pd_2dba_3 and P(*o*-tol)$_3$ in toluene at 120 °C. A polymer similar to **PT1** was previously prepared by Lai and co-workers via $FeCl_3$-mediated oxidative polymerization of 1,3-bis(3-alkylthienyl)azulene.[42] In that case, alkyl substitution at the 3-thienyl positions resulted in significant steric interactions between the thiophene groups and the azulene unit leading to deviation from coplanarity and decreased conjugation. To address this issue, we have specifically employed the bithiophene monomer **4** containing internal alkyl groups in order to minimize steric repulsion. All polymers were isolated in moderate to excellent yield (57–93%) after purification by filtration through silica and repeated precipitations

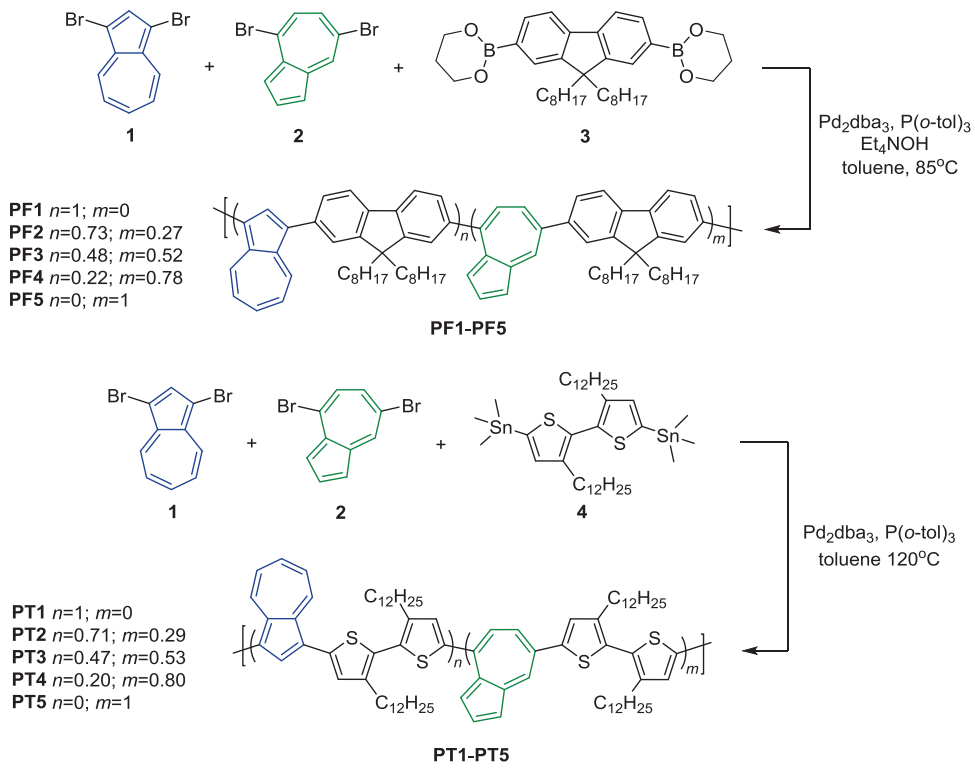

Scheme 2. Synthesis of polymer series **PF1**–**PF5** and **PT1**–**PT5** using various feed ratios of dibrominated azulene regioisomers **1** and **2**.

and were found to be fully soluble in common organic solvents such as THF, dichloromethane, and chloroform.

The polymers were characterized using ^{1}H NMR spectroscopy to determine composition and GPC to estimate molecular weight and molecular weight distribution (**Table 1**). The composition of the copolymers was found to closely match the feed ratios of the two regioisomeric azulene monomers. Unique sets of resonances are clearly observed for the protons on the azulene moiety according to the 1,3- or 4,7-substitution pattern, facilitating calculation of the repeating unit ratios based on relative integration values. For polymers **PF1**–**PF5**, resonances corresponding to the 1,3-disubstituted azulene repeat unit appear at 8.71–8.22 ppm while the resonances at 8.88–8.76 ppm correspond to the 4,7-disubstituted azulene unit (Figure S2). A similar differentiation of regioisomers was possible for polymers **PT1**–**PT5** with unique resonance at 8.36–8.18 ppm (1,3-disubstituted) and 8.03–7.72 ppm (4,7-disubstituted). For both polymer series, molecular weight was generally observed to increase with increasing feed ratio of 4,7-dibromoazulene **2**, which reflects the difference in reactivity between **1** and **2**. The more electron-deficient Ar–Br bond of 4,7-dibromoazulene **2** should favor oxidative addition of palladium and thus regioisomer **2** may have increased reactivity during polymerization when compared to **1**.

Table 1. Characterization results for polymer series **PF1**–**PF5** and **PT1**–**PT5**.

Polymer	Monomer feed ratio [1:2]	Experimental Ratio [*n*:*m*][a)]	M_n [kg mol^{-1}][b)]	M_w [kg mol^{-1}][b)]	M_w/M_n[b)]
PF1	100 : 0	—	10.5	17.3	1.6
PF2	75 : 25	73 : 27	9.8	20.6	2.1
PF3	50 : 50	48 : 52	17.7	34.8	2.0
PF4	25 : 75	22 : 78	19.3	42.8	2.2
PF5	0 : 100	—	34.3	73.3	2.1
PT1	100 : 0	—	7.5	12.0	1.6
PT2	75 : 25	71 : 29	6.0	7.9	1.3
PT3	50 : 50	47 : 53	6.4	8.2	1.3
PT4	25 : 75	20 : 80	8.0	11.1	1.4
PT5	0 : 100	—	21.0	34.9	1.6

a) Measured by ^{1}H NMR spectroscopy; b)Measured by GPC relative to PS standards.

The optical properties of the copolymers were initially investigated by UV–Visible absorption spectroscopy in chloroform with similar spectral characteristics to those of the model compounds being observed (**Figure 4**). It should be pointed out that absorptivity values of the copolymer solutions are based on concentration of repeating units. In the neutral state, the copolymers exhibit a gradual transition from a single, broad absorption for **PF1** and **PT1** to two distinct absorption peaks with increasing composition of 4,7-disubstituted azulene units; **PF5** exhibits absorption maxima at 327 and 402 nm while **PT5** has maxima at 316 and 422 nm. Attenuation of the broad absorption centered at approximately 650 nm corresponding to the S_0–S_1 transition of azulene is also observed with increasing incorporation of 1,3-disubstituted azulene units. The absorption spectra indicate that the effective conjugation length of the copolymers is relatively short, as a significant redshift in

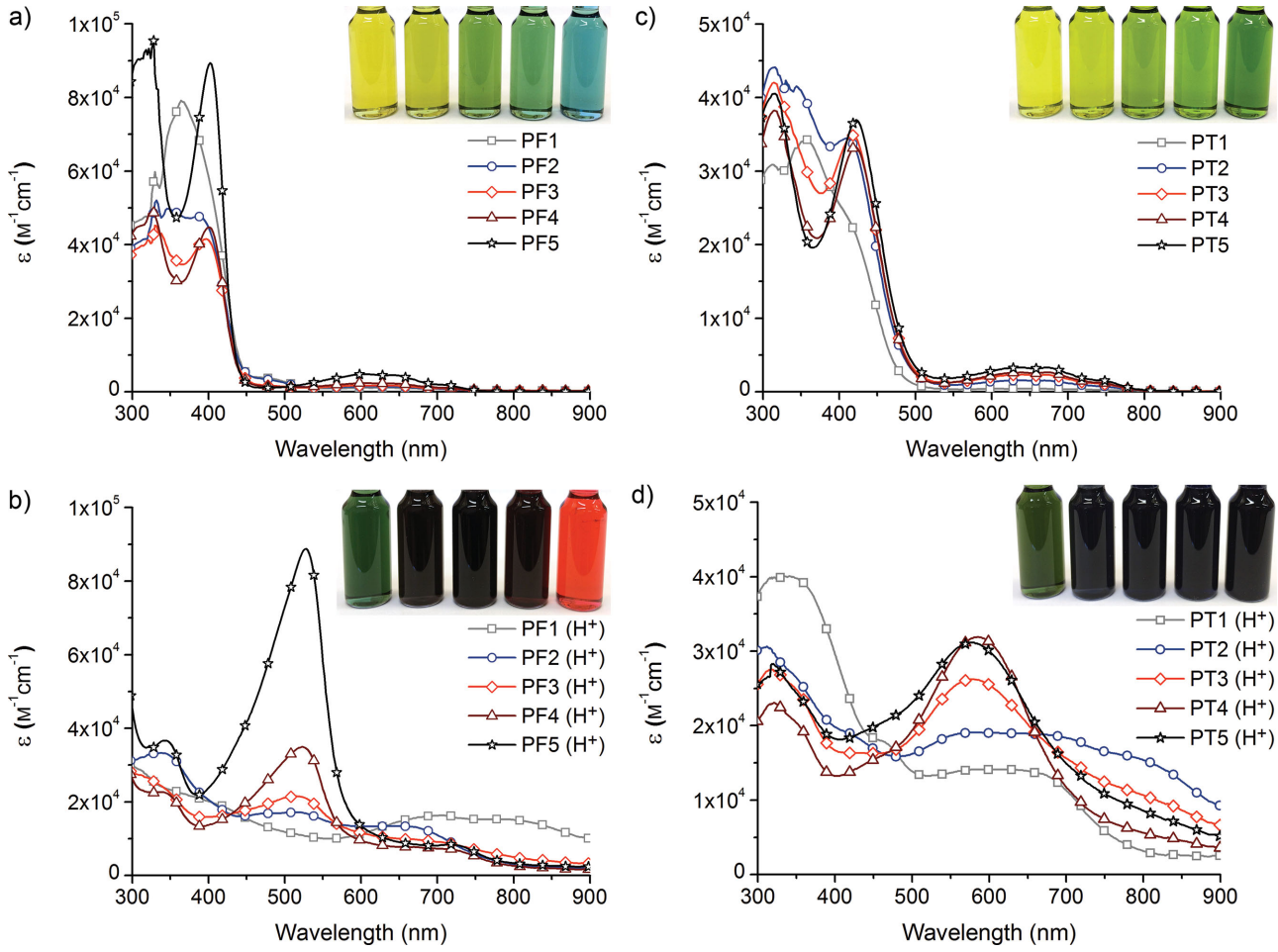

Figure 4. UV–Visible spectra of polymers **PF1**–**PF5** in a) $CHCl_3$, b) $CHCl_3$/TFA (30% TFA by volume) and **PT1**–**PT5** in c) $CHCl_3$, d) $CHCl_3$/TFA (30% TFA by volume). Insets show optical photographs of the polymer solutions with a repeating unit concentration of 1×10^{-4} M (from left to right: **PF1**–**PF5**, **PT1**–**PT5**).

the dominant absorption peak is absent when comparing the spectra of the copolymers to those of the corresponding model compounds in Figure 2. This observation is consistent with the DFT optimized structures that demonstrate deviation from coplanarity between the azulene units and neighboring groups. Qualitatively, the fluctuations in absorption for the polymer series are reflected in the change in their solution colors where the copolymers display a transition from yellow to blue for **PF1** to **PF5** and yellow to green for **PT1** to **PT5**, respectively.

Similar to the stimuli-responsive behavior of the model compounds, pronounced changes in the UV–Visible absorption spectra – and qualitatively, the color of the polymer solutions – are observed upon addition of TFA to the copolymers dissolved in chloroform (Figure 4). For the fluorene-containing polymers, addition of TFA results in the appearance of a peak at ~520 nm that gradually increases in intensity to reach a maximum optical density for **PF5** which contains exclusively 4,7-disubstituted azulene units. In contrast, **PF1** exhibits relatively weak absorbance, although it displays a very broad absorption profile that extends well into the near-IR region, presumably due to enhanced ICT that results from the dislocation of HOMO–LUMO orbitals with 1,3-disubstitued azulenium groups. Significantly, copolymers with intermediate composition, **PF2**–**PF4**, exhibit absorption spectra that extend past ~800 nm and the colors of their solutions are optically distinct from both **PF1** and **PF5**. Copolymers **PT1**–**PT5** incorporating bithiophene units also demonstrated a strong response to protonation with TFA, resulting in broad absorption from the UV to the near-IR region of the electromagnetic spectrum. An increase in the optical density around ~580 nm was observed with increasing incorporation of 4,7-disubstituted azulene units, while **PT2** incorporating approximately 71% 1,3-disubstituted azulene units exhibits the highest absorptivity at the longest wavelengths (>900 nm). These results demonstrate that the optoelectronic and responsive properties of the conjugated copolymers can be significantly modulated based on both the regiochemistry of azulene repeat units as well as the nature of the comonomer, in this case fluorene vs bithiophene.

The ability to 'switch on' the fluorescence of azulene-containing materials upon doping with strong acid is a unique capability with many important implications.[44] Azulene itself fluoresces weakly due to a dominant transition from the excited S_2 state to the S_0 state,[57,58] whereas the azulenium cation is strongly fluorescent in highly acidic environments.[59] In a

similar fashion, the conjugated copolymers exhibit dramatic changes in photoluminescence behavior upon protonation (**Figure 5**). Interestingly, a strong solvatochromic effect was also observed with significant emission occurring from THF solutions compared to only weak fluorescence of the polymers in chloroform. This is in direct contrast to the absorption measurements which demonstrated considerable spectroscopic response for chloroform solutions, but only minor changes in THF (Figure S3). Excitation at the absorption maxima of each polymer resulted in the strongest fluorescence response for polymers **PF1** and **PT1** containing exclusively 1,3-disubstituted azulene units. Like azulene, the copolymers are essentially non-emissive in their neutral state, but addition of TFA results in strong photoluminescence signals at approximately 420 and 480 nm for **PF1** and **PT1**, respectively. This corresponds to a markedly large Stokes shift of 155 nm for **PT1**. Attenuation of these fluorescence signals is observed with increasing incorporation of 4,7-disubstituted azulene units with a concomitant increase of the peak around 365 nm for **PT1**–**PT5** corresponding to emission of the bithiophene unit. It should be noted that our results differ from those of Xu and co-workers who previously reported polymer **PF1** to be non-fluorescent under similar conditions.[41]

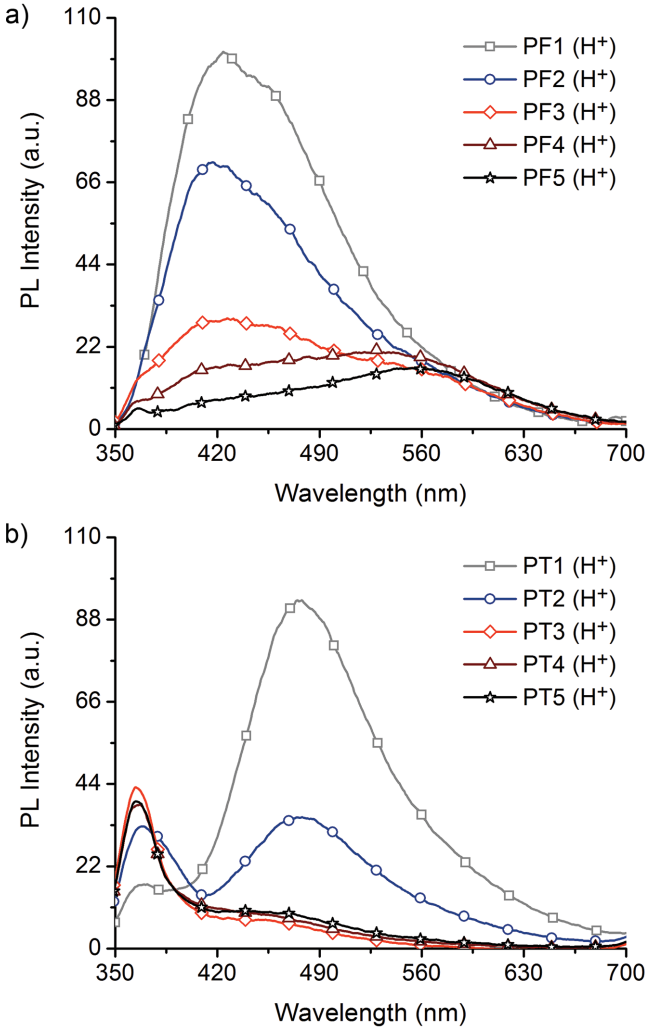

Figure 5. Fluorescence spectra of a) **PF1**–**PF5** and b) **PT1**–**PT5** in THF/TFA (30% TFA by volume). Polymers were excited at wavelengths corresponding to their absorption maxima (see Figure S3 for details).

The reversibility of the colorimetric response to TFA was investigated both in solution and in the solid state. The acid-mediated optical changes of many azulene-containing materials have been demonstrated to be reversible in solution, with the original spectral characteristics being recovered after neutralization of the protonated azulenium species.[34,44,45] Consistent with these observations, we found that the original properties of the copolymers could be recovered after neutralization of the acidic polymer solutions. Treatment of copolymers dissolved in chloroform containing 30% TFA with sodium carbonate followed be simple filtration through a cotton plug resulted in recovery of the neutral polymers exhibiting essentially identical absorption profiles to the materials prior to protonation (Figure S4). In order to transfer these stimuli-responsive properties to technological applications like sensors, we were interested to determine if the same colorimetric responses could be achieved in the solid state. To demonstrate this concept, thin films of polymer **PF5** were spin-coated from chlorobenzene onto glass substrates and exposed to TFA vapor within an enclosed chamber in an argon atmosphere. The films turned from green to red rapidly (within seconds, see Movie S1) and could be converted back to their neutral state (green color) by removing the TFA under a flow of argon. This process was repeated on the same polymer film for five consecutive cycles with minimal degradation in film color being observed (**Figure 6**). To further characterize this behavior, digital photographs of the thin film over the course of the cycling experiment were subjected to a colorimetric evaluation by monitoring the changes in RGB (red, green, blue) color levels similar to previously reported methods.[60,61] Changes in the green component as a function of cycle number are shown in Figure 6 while variation in the red and blue channels as well as the photographs of the thin

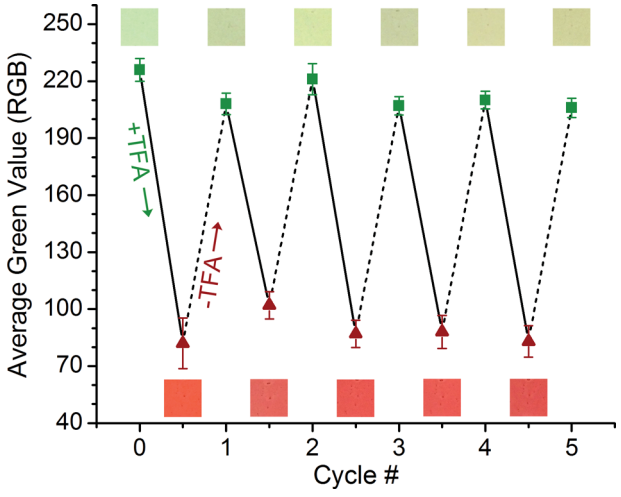

Figure 6. RGB color analysis (green channel) of the reversible protonation/deprotonation of a thin film of **PF5** spin-coated on glass over five complete cycles (exposure to TFA vapor followed by removal of TFA under a flow of argon). The colored squares above and below the data points are actual images of the thin film at each step.

film are shown in the Supporting Information (Figure S5 and Figure S6, respectively). Interestingly, the polymer films also exhibit reversible color switching behavior under ambient conditions without efforts to preclude oxygen; however, under these conditions accelerated degradation in film color was observed which is likely due to irreversible oxidation of the azulenium cations (Figure S7).[62,63]

3. Conclusions

Two series of random conjugated polymers were prepared that incorporate varying ratios of regioisomeric azulene units connected via the 5-membered or 7-membered ring. The optoelectronic and stimuli-responsive properties of the materials can be systematically modulated by tuning the composition of the polymers and the relative percentage of azulene regioisomers along the polymer chain. UV–Visible absorption measurements and DFT calculations reveal that the substitution pattern of the azulene repeat unit and the nature of the substituents have a strong influence on the resulting polymer properties. Fluorescence of the materials can also be 'turned on' upon protonation with a markedly large Stokes shift of 155 nm observed for bithiophene-containing polymer **PT1**. Significantly, the colorimetric response of the polymers upon exposure to trifluoroacetic acid was shown to be reversible in the solid state with thin films of polymer **PF5** spin-coated on glass undergoing rapid and reversible color switching. Ultimately, this work represents a new design strategy in which the optoelectronic properties of conjugated polymers can be dramatically altered by simply varying the regiochemistry of the constituent building blocks along the polymer backbone.

4. Experimental Section

Materials: All reagents from commercial sources were used without further purification unless otherwise stated. Deuterated solvents were obtained from Cambridge Isotope Laboratories, Inc. The 9,9-dioctylfluorene-2,7-bis(trimethylborate) **3** was purchased from Aldrich and purified by recrystallization from acetone prior to use. The 1,3-dibromoazulene **1**,[53] 4,7-dibromoazulene **2**,[44] 2-(9,9-dioctyl-9*H*-fluoren-2-yl)-4,4,5,5-tetramethyl-1,3,2-dioxaborolane,[64] 2-bromo-3,3′-didodecyl-2,2′-bithiophene,[65] and 5,5′-bis(trimethylstannyl)-3,3′-didodecyl-2,2′-bithiophene **4**[66] were prepared according to the literature procedures.

Instrumentation: NMR spectra were recorded using a Varian 500 or 600 MHz spectrometer. All ^{1}H NMR experiments are reported in δ units, parts per million (ppm), and were measured relative to the signals for residual chloroform (7.26 ppm) in deuterated solvent. All ^{13}C NMR spectra were measured in deuterated solvents and are reported in ppm relative to the signals for residual chloroform (77.16 ppm). Gel permeation chromatography (GPC) was performed on a Waters 2690 separation module equipped with Waters 2414 refractive index and 2996 photodiode array detectors using $CHCl_3$ containing 0.25% triethylamine as eluent at a flow rate of 1 mL/min. Molecular weights and molecular weight distributions were calculated relative to linear PS standards. Mass spectrometry was performed on a Waters GCT Premier time-of-flight mass spectrometer. Fluorescence spectra were recorded on a Varian Cary Eclipse fluorescence spectrometer. UV–Visible spectra were recorded on a Shimadzu UV 3600 spectrophotometer. IR spectra were recorded on a Perkin Elmer Spectrum 100 with a Universal ATR sampling accessory.

Synthesis of 2-(3,3′-Didodecyl-[2,2′-bithiophen]-5-yl)-4,4,5,5-tetramethyl-1,3,2-dioxaborolane: A 100 mL round-bottom flask equipped with a stir bar was charged with 2-bromo-3,3′-didodecyl-2,2′-bithiophene (0.802 g, 1.38 mmol) and THF (30 mL) and sealed with a septum. The flask was purged with argon for approximately 5 min and cooled with stirring to –78 °C. A 2.5 M solution of *n*-butyllithium in hexane (0.82 mL, 2.1 mmol) was added dropwise via syringe. The solution was stirred at –78 °C for 1 h followed by the addition of 2-isopropoxy-4,4,5,5-tetramethyl-1,3,2-dioxaborolane (0.49 mL, 2.3 mmol) in one portion. After stirring for 1 h at –78 °C the mixture was warmed to room temperature and stirred overnight. The resulting mixture was poured into water and extracted with ethyl acetate (100 mL). The organic layer was washed with water (2 × 50 mL), brine (50 mL), and the organic extract was dried over $MgSO_4$. The crude product was purified by flash chromatography on silica gel using ethyl acetate/hexane (1:1) as eluent to provide the title compound as a colorless liquid after drying under vacuum (810 mg, 93%). ^{1}H NMR (600 MHz, $CDCl_3$) δ: 0.88 (t, J = 7.0 Hz, 6H), 1.18–1.33 (m, 36H), 1.35 (s, 12H), 1.47–1.59 (m, 4H), 2.49 (m, 4H), 6.96 (d, J = 5.2 Hz, 1H), 7.28 (d, J = 5.1 Hz, 1H), 7.50 (s, 1H) ppm; ^{13}C NMR (125 MHz, $CDCl_3$) δ: 14.3, 22.9, 24.9, 28.9, 29.0, 29.5, 29.5, 29.6, 29.6, 29.6, 29.7, 29.8, 29.8, 29.8, 30.8, 32.1, 84.2, 125.5, 128.7, 128.8, 136.6, 138.9, 142.3, 143.9 ppm (some peaks overlap); IR ($CHCl_3$, cm^{-1}): 2924, 2854, 1466, 1419, 1382, 1329, 1296, 1269, 1143, 850, 575; HRMS (EI, m/z): calcd for $[C_{38}H_{65}BO_2S_2]^+$ (M^+), 627.4555; found, 627.4531.

Synthesis of 1,3-Bis(9,9-dioctylfluoren-2-yl)azulene, **MF1**: To a Schlenk flask equipped with a stir bar was added 1,3-dibromoazulene **1** (0.10 g, 0.35 mmol), 2-(9,9-dioctyl-9*H*-fluoren-2-yl)-4,4,5,5-tetramethyl-1,3,2-dioxaborolane (0.90 g, 1.7 mmol), $Pd(PPh_3)_4$ (20 mg, 17 μmol), and three drops of Aliquot 336. The vessel was sealed and evacuated/backfilled with argon three times followed by the addition of dry toluene (8 mL) and a degassed 2 M aqueous solution of Na_2CO_3 (7.0 mL, 14 mmol) via syringe. The mixture was heated at 110 °C for 24 h. After cooling, the organic layer was separated, concentrated, and redissolved in $CHCl_3$ (30 mL). This solution was washed with 2 M HCl (30 mL) then brine (2 × 30 mL), and the combined organic extracts were dried over anhydrous $MgSO_4$. The crude product was purified by chromatography on silica gel using hexane as eluent to provide the title compound as a green, tacky solid after drying under vacuum (270 mg, 85%). ^{1}H NMR (600 MHz, $CDCl_3$) δ: 0.65–0.78 (m, 8H), 0.80 (t, J = 7.2 Hz, 12H), 1.03–1.16 (m, 32H), 1.16–1.24 (m, 8H), 2.02 (dt, J = 11.2, 5.5 Hz, 8H), 7.11 (t, J = 9.7 Hz, 2H), 7.29–7.33 (m, 2H), 7.33–7.39 (m, 4H), 7.59 (t, J = 9.8 Hz, 1H), 7.62 (d, J = 1.5 Hz, 2H), 7.65 (dd, J = 7.7, 1.5 Hz, 2H), 7.76 (d, J = 7.2 Hz, 2H), 7.84 (d, J = 7.7 Hz, 2H), 8.26 (s, 1H), 8.58 (d, J = 9.7 Hz, 2H) ppm; ^{13}C NMR (125 MHz, $CDCl_3$) δ: 14.2, 22.7, 24.1, 29.4, 30.3, 31.9, 40.6, 55.3, 119.8, 120.0, 123.0, 123.5, 124.5, 126.9, 127.0, 128.7, 131.4, 135.9, 136.5, 137.0, 137.3, 139.2, 139.8, 141.1, 151.1, 151.3 ppm; IR (solid, cm^{-1}): 3055, 3019, 2954, 2923, 2851, 1568, 1454, 1365, 1295, 1264, 1154, 1004, 943, 875, 831, 780, 737, 678; MS (FD, m/z) calcd for $[C_{68}H_{88}]^+$ (M^+), 904.69; found, 904.64.

Synthesis of 4,7-Bis(9,9-dioctylfluoren-2-yl)azulene, **MF2**: Following a similar procedure as MF1, 4,7-dibromoazulene **2** (51 mg, 0.18 mmol), 2-(9,9-dioctyl-9*H*-fluoren-2-yl)-4,4,5,5-tetramethyl-1,3,2-dioxaborolane (0.45 g, 0.87 mmol), $Pd(PPh_3)_4$ (10 mg, 8.7 μmol), and two drops of Aliquot 336 were added to a Schlenk flask equipped with a stir bar. The vessel was sealed and evacuated/backfilled with argon three times followed by the addition of dry toluene (5 mL) and a degassed 2 M aqueous solution of Na_2CO_3 (3.5 mL, 7.0 mmol) via syringe. The mixture was heated at 110 °C for 24 h. The crude product was purified by column chromatography using hexane as eluent to provide the title compound as a blue, tacky solid after drying under vacuum (140 mg, 86%). ^{1}H NMR (600 MHz, $CDCl_3$) δ: 0.65–0.79 (m, 8H), 0.82 (dt, J = 9.5, 7.2 Hz, 12H), 1.03–1.18 (m, 32H), 1.18–1.28 (m, 8H), 1.96–2.10 (m, 8H), 7.23 (d, J = 3.3 Hz, 1H), 7.31–7.44 (m, 7H), 7.57 (dd, J = 3.7, 1.5 Hz, 1H), 7.62–7.72 (m, 4H), 7.77 (d, J = 7.3 Hz, 1H), 7.80 (d, J = 7.3 Hz, 1H), 7.82 (d, J = 7.8 Hz, 1H), 7.86 (d, J = 7.7 Hz, 1H), 7.88 (t, J = 3.8 Hz, 1H), 7.99 (dd, J = 10.8, 2.0 Hz, 1H), 8.80 (d, J = 2.0 Hz, 1H) ppm; ^{13}C NMR (125 MHz, $CDCl_3$) δ: 14.2, 14.2, 22.8, 22.8, 24.0, 24.0, 29.4, 29.4, 29.4, 29.9, 30.2, 31.9, 32.0, 40.5, 40.5, 55.4, 118.7, 119.6, 119.9, 120.0, 120.1,

120.5, 122.7, 123.1, 124.3, 125.8, 127.0, 127.0, 127.1, 127.3, 127.4, 128.2, 135.6, 136.6, 136.9, 137.6, 138.1, 140.3, 140.6, 140.8, 140.9, 141.3, 142.4, 143.6, 150.1, 150.7, 151.2, 151.3, 151.7 ppm (some peaks overlap); IR (solid, cm^{-1}): 3063, 30115, 2954, 2923, 2851, 1519, 1446, 1375, 1302, 1264, 1004, 991, 932, 889, 821, 781, 756, 739, 665; MS (FD, *m*/*z*) calcd for $[C_{68}H_{88}]^+$ (M^+), 904.69; found, 904.81.

Synthesis of 1,3-Bis(3,3′-didodecyl-[2,2′-bithiophen]-5-yl)azulene, **MT3**: A mixture of 1,3-dibromoazulene **1** (0.10 g, 0.35 mmol), 2-(3,3′-didodecyl-[2,2′-bithiophen]-5-yl)-4,4,5,5-tetramethyl-1,3,2-dioxaborolane (0.44 g, 0.70 mmol), $Pd(PPh_3)_4$ (4.0 mg, 0.035 mmol), and three drops of Aliquot 336 were combined in a Schlenk flask equipped with a stir bar. The vessel was sealed and evacuated/backfilled with argon three times followed by the addition of dry toluene and a degassed 1 M aqueous solution of Na_2CO_3 (1.0 mL, 1.0 mmol) via syringe. The mixture was heated at 110 °C for 24 h. After cooling, the organic layer was separated, concentrated, and redissolved in $CHCl_3$ (30 mL). This solution was washed with 2 M HCl (30 mL) then brine (2 × 30 mL), and the combined organic extracts were dried over anhydrous $MgSO_4$. The crude product was purified by chromatography on silica gel using hexane as eluent to provide the title compound as a green solid after drying under vacuum (260 mg, 66%). ^{1}H NMR (600 MHz, $CDCl_3$) δ: 0.83–0.92 (m, 12H), 1.18–1.36 (m, 72H), 1.57–1.68 (m, 8H), 2.58 (t, J = 7.8 Hz, 4H), 2.61 (t, J = 7.6 Hz, 4H), 7.00 (d, J = 5.2 Hz, 2H), 7.16 (t, J = 9.8 Hz, 2H), 7.18 (s, 2H), 7.31 (d, J = 5.2 Hz, 2H), 7.58 (t, J = 9.7 Hz, 1H), 8.20 (s, 1H), 8.75 (d, J = 9.7 Hz, 2H) ppm; ^{13}C NMR (125 MHz, $CDCl_3$) δ: 14.3, 14.3, 22.8, 22.9, 29.1, 29.2, 29.5, 29.5, 29.6, 29.6, 29.7, 29.8, 29.8, 29.8, 29.8, 29.9, 31.0, 31.0, 32.1, 32.1, 123.3, 124.4, 125.4, 126.7, 128.3, 128.8, 129.0, 136.6, 136.7, 137.0, 138.4, 139.8, 142.5, 143.1 ppm (some peaks overlap); IR (solid, cm^{-1}): 3063, 2912, 2848, 1564, 1470, 1402, 1376, 1301, 1232, 1191, 1085, 944, 917, 872, 829, 730, 716, 683; MS (FD, *m*/*z*) calcd for $[C_{74}H_{112}S_4]^+$ (M^+), 1128.76; found, 1128.86.

Synthesis of 4,7-Bis(3,3′-didodecyl-2,2′-bithyenyl)azulene, **MT4**: Following a similar procedure as MT3, 4,7-dibromoazulene **2** (42 mg, 0.15 mmol), 2-(3,3′-didodecyl-[2,2′-bithiophen]-5-yl)-4,4,5,5-tetramethyl-1,3,2-dioxaborolane (0.28 g, 0.45 mmol), $Pd(PPh_3)_4$ (8.2 mg, 5.5 µmol), and two drops of Aliquot 336 were added to a Schlenk flask equipped with a stir bar. The vessel was sealed and evacuated/backfilled with argon three times followed by the addition of dry toluene (5 mL) and a degassed 2 M aqueous solution of Na_2CO_3 (2.2 mL, 4.4 mmol) via syringe. The mixture was heated at 110 °C for 24 h. The crude product was purified by chromatography on silica gel using hexane as eluent to provide the title compound as a dark green, tacky solid after drying under vacuum (120 mg, 71%). ^{1}H NMR (600 MHz, $CDCl_3$) δ: 0.82–0.90 (m, 12H), 1.18–1.35 (m, 72H), 1.56–1.65 (m, 8H), 2.54 (t, J = 7.9 Hz, 2H), 2.61 (dt, J = 16.3, 7.8 Hz, 6H), 6.99 (d, J = 5.5 Hz, 1H), 7.01 (d, J = 5.0 Hz, 1H), 7.29 (s, 1H), 7.32 (d, J = 5.3 Hz, 1H), 7.34 (d, J = 5.2 Hz, 1H), 7.42 (d, J = 11.0 Hz, 1H), 7.46 (s, 1H), 7.49 (d, J = 3.6 Hz, 1H), 7.74 (d, J = 3.7 Hz, 1H), 7.88 (t, J = 3.8 Hz, 1H), 7.92 (dd, J = 11.1, 2.1 Hz, 1H), 8.72 (s, 1H) ppm; ^{13}C NMR (125 MHz, $CDCl_3$) δ: 14.3, 14.3, 22.8, 22.9, 29.1, 29.1, 29.2, 29.3, 29.5, 29.5, 29.6, 29.6, 29.7, 29.7, 29.8, 29.8, 29.8, 29.8, 29.8, 29.8, 29.8, 29.9, 30.9, 31.0, 32.1, 32.1, 119.3, 121.7, 125.5, 125.6, 125.7, 127.8, 128.4, 128.7, 128.8, 128.9, 129.2, 130.3, 131.0, 133.6, 135.6, 136.3, 137.6, 140.5, 141.2, 142.6, 142.7, 142.7, 144.0, 144.3, 146.6 ppm (some peaks overlap); IR (solid, cm^{-1}): 3067, 2920, 2851, 1516, 1463, 1418, 1376, 1218, 1185, 1070, 990, 916, 882, 832, 754, 719; MS (FD, *m*/*z*) calcd for $[C_{74}H_{112}S_4]^+$ (M^+), 1128.76; found, 1128.87.

Representative Procedure for Polymerizations by Suzuki-Miyaura Cross-Coupling (PF1–PF5): A detailed procedure is provided for polymer **PF3**. A mixture of 1,3-dibromoazulene **1** (25.0 mg, 0.0874 mmol), 4,7-dibromoazulene **2** (25.0 mg, 0.0874 mmol), 9,9-dioctylfluorene-2,7-bis(trimethylborate) **3** (97.6 mg, 0.175 mmol), Pd_2dba_3 (5.6 mg, 6.0 µmol), and P(*o*-tol)$_3$ (4.3 mg, 14 µmol) were combined in a 10 mL Schlenk flask equipped with a stir bar and septum. The vessel was evacuated and backfilled with argon three times followed by the addition of degassed toluene (5 mL) and 20% aqueous solution of tetraethylammonium hydroxide (0.8 mL) via syringe. The resulting solution was heated at 85 °C under argon for 48 h. The mixture was cooled to room temperature, eluted through a short pad of silica gel using $CHCl_3$ as eluent and poured into methanol (150 mL). The precipitate was collected by filtration using a 0.45 µm nylon membrane and washed consecutively with methanol, water, acetone, and hexanes. The polymer was dissolved in a small amount of chloroform and precipitated a second time into methanol, providing the title compound as a green solid after filtration and drying under vacuum (76 mg, 84%). ^{1}H NMR (600 MHz, $CDCl_3$) δ: 0.67–1.00 (br m), 1.02–1.31 (br m), 1.95–2.24 (br m), 7.07–7.22 (br m), 7.27–7.33 (br m), 7.35–7.40 (br m), 7.41–7.54 (br m), 7.54–7.82 (br m), 7.82–7.98 (br m), 7.98–8.11 (br m), 8.26–8.36 (br m), 8.36–8.43 (br m), 8.43–8.50 (br m), 8.55–8.69 (br m), 8.78–8.89 (br m) ppm; GPC ($CHCl_3$): M_n = 17.7 kg mol^{-1}; M_w/M_n = 2.0.

Representative Procedure for Polymerizations by Stille Cross-Coupling (PT1–PT5): A detailed procedure is provided for polymer **PT3**. A mixture of 1,3-dibromoazulene **1** (25.0 mg, 0.0874 mmol), 4,7-dibromoazulene **2** (25.0 mg, 0.0874 mmol), 5,5′-bis(trimethylstannyl)-3,3′-didodecyl-2,2′-bithiophene **4** (0.145 g, 0.175 mmol), Pd_2dba_3 (5.6 mg, 6.0 µmol) and P(*o*-tol)$_3$ (4.3 mg, 14 µmol) were combined in a 10 mL Schlenk flask equipped with a stir bar and septum. The vessel was evacuated and backfilled with argon three times followed by the addition of degassed toluene (4 mL) via syringe. The resulting solution was heated at 120 °C under argon for 48 h. The mixture was cooled to room temperature, eluted through a short pad of silica gel using $CHCl_3$ as eluent, and poured into methanol (150 mL). The precipitate was collected by filtration using a 0.45 µm nylon membrane and washed consecutively with methanol, acetone, and hexanes. The polymer was dissolved in a small amount of chloroform and precipitated a second time into methanol, providing the title compound as a green solid after filtration and drying under vacuum (80 mg, 73%). ^{1}H NMR (600 MHz, $CDCl_3$) δ: 0.78–0.92 (br m), 1.12–1.45 (br m), 1.64–1.77 (br m), 2.51–2.78 (br m), 6.97–7.03 (br m), 7.07–7.13 (br m), 7.13–7.26 (br m), 7.29–7.38 (br m), 7.40–7.55 (br m), 7.55–7.69 (br m), 7.72–7.83 (br m), 7.85–8.01 (br m), 8.03–8.07 (br m), 8.19–8.29 (br m), 8.28–8.38 (br m), 8.68–8.85 (br m) ppm; GPC ($CHCl_3$): M_n = 6.4 kg mol^{-1}; M_w/M_n = 1.3.

Supporting Information

Supporting Information is available from the Wiley Online Library or from the author.

Acknowledgements

The authors thank the MRSEC program of the National Science Foundation (Award No. DMR–1121053) for partial financial support. M.J.R. gratefully acknowledges funding from UC Regents, CSP Technologies, and the DOE Office of Science Graduate Fellowship Program (DOE-SCGF, administered by ORISE-ORAU under Contract No. DE–AC05–06OR23100). M.M. thanks the JSPS Research Fellowships for Young Scientists.

Received: July 29, 2014
Revised: August 24, 2014
Published online: September 12, 2014

[1] L. Bian, E. Zhu, J. Tang, W. Tang, F. Zhang, *Prog. Polym. Sci.* **2012**, *37*, 1292.
[2] A. Facchetti, *Chem. Mater.* **2011**, *23*, 733.
[3] P.-L. T. Boudreault, A. Najari, M. Leclerc, *Chem. Mater.* **2011**, *23*, 456.
[4] F. Liu, Z. A. Page, V. V. Duzhko, T. P. Russell, T. Emrick, *Adv. Mater.* **2013**, *25*, 6868.
[5] H. Sirringhaus, *Adv. Mater.* **2014**, *26*, 1319.
[6] Y. Mei, M. A. Loth, M. Payne, W. Zhang, J. Smith, C. S. Day, S. R. Parkin, M. Heeney, I. McCulloch, T. D. Anthopoulos, J. E. Anthony, O. D. Jurchescu, *Adv. Mater.* **2013**, *25*, 4352.

[7] A. C. Grimsdale, K. Leok Chan, R. E. Martin, P. G. Jokisz, A. B. Holmes, *Chem. Rev.* **2009**, *109*, 897.
[8] M. J. Robb, S.-Y. Ku, F. G. Brunetti, C. J. Hawker, *J. Polym. Sci. A Polym. Chem.* **2013**, *51*, 1263.
[9] A. J. Kronemeijer, E. Gili, M. Shahid, J. Rivnay, A. Salleo, M. Heeney, H. Sirringhaus, *Adv. Mater.* **2012**, *24*, 1558.
[10] S. Qu, H. Tian, *Chem. Commun.* **2012**, *48*, 3039.
[11] A. B. Tamayo, B. Walker, T.-Q. Nguyen, *J. Phys. Chem. C* **2008**, *112*, 11545.
[12] Z. Chen, M. J. Lee, R. S. Ashraf, Y. Gu, S. Albert-Seifried, M. M. Nielsen, B. Schroeder, T. D. Anthopoulos, M. Heeney, I. McCulloch, H. Sirringhaus, *Adv. Mater.* **2012**, *24*, 647.
[13] P. P. Khlyabich, B. Burkhart, C. F. Ng, B. C. Thompson, *Macromolecules* **2011**, *44*, 5079.
[14] J. Mei, K. R. Graham, R. Stalder, J. R. Reynolds, *Org. Lett.* **2010**, *12*, 660.
[15] E. Wang, W. Mammo, M. R. Andersson, *Adv. Mater.* **2014**, *26*, 1801.
[16] R. Stalder, J. Mei, K. R. Graham, L. A. Estrada, J. R. Reynolds, *Chem. Mat.* **2014**, *26*, 664.
[17] Y. Zou, A. Najari, P. Berrouard, S. Beaupré, B. Réda Aïch, Y. Tao, M. Leclerc, *J. Am. Chem. Soc.* **2010**, *132*, 5330.
[18] P. Berrouard, S. Dufresne, A. Pron, J. Veilleux, M. Leclerc, *J. Org. Chem.* **2012**, *77*, 8167.
[19] P. Berrouard, A. Najari, A. Pron, D. Gendron, P.-O. Morin, J.-R. Pouliot, J. Veilleux, M. Leclerc, *Angew. Chem. Int. Ed.* **2012**, *51*, 2068.
[20] Y. Zhang, S. K. Hau, H.-L. Yip, Y. Sun, O. Acton, A. K.-Y. Jen, *Chem. Mater.* **2010**, *22*, 2696.
[21] Z. Ma, E. Wang, M. E. Jarvid, P. Henriksson, O. Inganäs, F. Zhang, M. R. Andersson, *J. Mater. Chem.* **2012**, *22*, 2306.
[22] C. Cabanetos, A. El Labban, J. A. Bartelt, J. D. Douglas, W. R. Mateker, J. M. J. Fréchet, M. D. McGehee, P. M. Beaujuge, *J. Am. Chem. Soc.* **2013**, *135*, 4656.
[23] P. Foggi, F. V. R. Neuwahl, L. Moroni, P. R. Salvi, *J. Phys. Chem. A* **2003**, *107*, 1689.
[24] J. Michl, E. W. Thulstrup, *Tetrahedron* **1976**, *32*, 205.
[25] R. S. H. Liu, *J. Chem. Educ.* **2002**, *79*, 183.
[26] E. Puodziukynaite, H.-W. Wang, J. Lawrence, A. J. Wise, T. P. Russell, M. D. Barnes, T. Emrick, *J. Am. Chem. Soc.* **2014**, *136*, 11043.
[27] Y. Yamaguchi, K. Ogawa, K. Nakayama, Y. Ohba, H. Katagiri, *J. Am. Chem. Soc.* **2013**, *135*, 19095.
[28] J. Xia, B. Capozzi, S. Wei, M. Strange, A. Batra, J. R. Moreno, R. J. Amir, E. Amir, G. C. Solomon, L. Venkataraman, L. M. Campos, *Nano Lett.* **2014**, *14*, 2941.
[29] M. Murai, S.-Y. Ku, N. D. Treat, M. J. Robb, M. L. Chabinyc, C. J. Hawker, *Chem. Sci.* **2014**, *5*, 3753.
[30] D. T. McQuade, A. E. Pullen, T. M. Swager, *Chem. Rev.* **2000**, *100*, 2537.
[31] D. Gopalakrishnan, W. R. Dichtel, *J. Am. Chem. Soc.* **2013**, *135*, 8357.
[32] D. Wang, X. Gong, P. S. Heeger, F. Rininsland, G. C. Bazan, A. J. Heeger, *Proc. Natl. Acad. Sci. USA* **2002**, *99*, 49.
[33] S. S. Danyluk, W. G. Schneider, *Can. J. Chem.* **1962**, *40*, 1777.
[34] M. Koch, O. Blacque, K. Venkatesan, *Org. Lett.* **2012**, *14*, 1580.
[35] F. Wang, T. T. Lin, C. He, H. Chi, T. Tang, Y.-H. Lai, *J. Mater. Chem.* **2012**, *22*, 10448.
[36] T. Tang, T. Lin, F. Wang, C. He, *Polym. Chem.* **2014**, *5*, 2980.
[37] F. Wang, Y.-H. Lai, N. M. Kocherginsky, Y. Y. Kosteski, *Org. Lett.* **2003**, *5*, 995.
[38] F. Wang, Y.-H. Lai, *Macromolecules* **2003**, *36*, 536.
[39] M. Iyoda, K. Sato, M. Oda, *Tetrahedron Lett.* **1985**, *26*, 3829.
[40] F. Wang, Y.-H. Lai, M. Y. Han, *Org. Lett.* **2003**, *5*, 4791.
[41] X. Wang, J. K.-P. Ng, P. Jia, T. Lin, C. M. Cho, J. Xu, X. Lu, C. He, *Macromolecules* **2009**, *42*, 5534.
[42] F. Wang, Y.-H. Lai, M.-Y. Han, *Macromolecules* **2004**, *37*, 3222.
[43] E. J. Dell, L. M. Campos, *J. Mater. Chem.* **2012**, *22*, 12945.
[44] E. Amir, R. J. Amir, L. M. Campos, C. J. Hawker, *J. Am. Chem. Soc.* **2011**, *133*, 10046.
[45] M. Murai, E. Amir, R. J. Amir, C. J. Hawker, *Chem. Sci.* **2012**, *3*, 2721.
[46] B. Burkhart, P. P. Khlyabich, T. Cakir Canak, T. W. LaJoie, B. C. Thompson, *Macromolecules* **2011**, *44*, 1242.
[47] A. E. Rudenko, C. A. Wiley, S. M. Stone, J. F. Tannaci, B. C. Thompson, *J. Polym. Sci. A Polym. Chem.* **2012**, *50*, 3691.
[48] H. Li, F. Liu, X. Wang, C. Gu, P. Wang, H. Fu, *Macromolecules* **2013**, *46*, 9211.
[49] J. Li, K.-H. Ong, P. Sonar, S.-L. Lim, G.-M. Ng, H.-K. Wong, H.-S. Tan, Z.-K. Chen, *Polym. Chem.* **2013**, *4*, 804.
[50] K. Li, P. P. Khlyabich, L. Li, B. Burkhart, B. C. Thompson, J. C. Campbell, *J. Phys. Chem. C* **2013**, *117*, 6940.
[51] J. Zhou, S. Xie, E. F. Amond, M. L. Becker, *Macromolecules* **2013**, *46*, 3391.
[52] A. E. Rudenko, P. P. Khlyabich, B. C. Thompson, *ACS Macro Lett.* **2014**, *3*, 387.
[53] A. G. Anderson, J. A. Nelson, J. J. Tazuma, *J. Am. Chem. Soc.* **1953**, *75*, 4980.
[54] N. J. Turro, V. Ramamurthy, W. Cherry, W. Farneth, *Chem. Rev.* **1978**, *78*, 125.
[55] J. W. Sidman, D. S. McClure, *J. Chem. Phys.* **1956**, *24*, 757.
[56] R. Stalder, J. Mei, J. Subbiah, C. Grand, L. A. Estrada, F. So, J. R. Reynolds, *Macromolecules* **2011**, *44*, 6303.
[57] M. Beer, H. C. Longuet-Higgins, *J. Chem. Phys.* **1955**, *23*, 1390.
[58] G. Viswanath, M. Kasha, *J. Chem. Phys.* **1956**, *24*, 574.
[59] K. H. Grellmann, E. Heilbronner, P. Seiler, A. Weller, *J. Am. Chem. Soc.* **1968**, *90*, 4238.
[60] L. D. Bonifacio, D. P. Puzzo, S. Breslav, B. M. Willey, A. McGeer, G. A. Ozin, *Adv. Mater.* **2010**, *22*, 1351.
[61] M. C. Janzen, J. B. Ponder, D. P. Bailey, C. K. Ingison, K. S. Suslick, *Anal. Chem.* **2006**, *78*, 3591.
[62] G. Nöll, C. Lambert, M. Lynch, M. Porsch, J. Daub, *J. Phys. Chem. C* **2008**, *112*, 2156.
[63] K. Tanaka, M. Toriumi, S. Wang, T. Yamabe, *Polym. J.* **1990**, *22*, 1001.
[64] M. Belletête, S. Beaupré, J. Bouchard, P. Blondin, M. Leclerc, G. Durocher, *J. Phys. Chem. B* **2000**, *104*, 9118.
[65] R. Kiselev, S.-H. Yoon, H. Choi, J.-M. Lee (Lg Chem, Ltd) US Patent Appl. 20100236631 A1, **2007**.
[66] W. Yue, Y. Zhao, H. Tian, D. Song, Z. Xie, D. Yan, Y. Geng, F. Wang, *Macromolecules* **2009**, *42*, 6510.